International Journal of Reliability, Risk and Safety: Theory and Application

Online ISSN: 2676-3346

OPEN ACCESS

Vol. 9/ Issue 1/ 2026/ pp. 42-55

DOI: 10.22034/IJRRS.2026.9.1.4

Received: 01 August 2025, Revised: 28 January 2026, Accepted: 09 May 2026

Available online at: https://www.ijrrs.com

Original Research Article

Integrating Structural Uncertainty into Demand and Capacity Factored Design: A Case Study of Existing Moment-Resisting Steel Structures

Sasan Motaghed [1*] and Vahid Barzian [2]

1. Department of Civil Engineering, Faculty of Civil engineering and architecture, Shahid Chamran University of Ahvaz, Ahvaz, Iran

2. Faculty of Engineering, Behbahan Khatam Alanbia University of Technology, Behbahan, Iran

*** s.motaghed@scu.ac.ir**

Abstract

Quantitative assessment of seismic performance is vital for establishing the safety and reliability of structural systems, especially in high-hazard regions. This study employs the probabilistic Demand Capacity Factored Design (DCFD) framework, integrating structural uncertainty, to evaluate the seismic safety of 12 medium-ductility steel moment-resisting frames designed according to the third (ASD) and fourth (LRFD) editions of the Iranian seismic code (Standard No. 2800) and the Iranian National Building Codes. The frames, varying in height (3, 5, and 8 stories) and bay count (3 and 5 bays), represent typical residential buildings modeled in OpenSees and subjected to Incremental Dynamic Analysis (IDA) using 20 carefully selected ground motion records. Key uncertainties in demand and capacity are explicitly quantified following FEMA guidelines. Seismic performance is evaluated at Life Safety (LS, 10% APE in 50 years) and Collapse Prevention (CP, 2% APE in 50 years) levels. Results demonstrate that structures designed per the fourth code edition consistently achieve superior seismic performance and higher reliability indices than those designed per the third edition, owing to more robust drift limits and response modification factors. At the CP level, all frames meet safety objectives, while at the LS level, taller and more complex frames require fourth edition provisions to ensure reliability targets. These findings highlight the effectiveness of the DCFD framework, combined with IDA, for comprehensive, uncertainty-aware seismic safety assessment and underscore the enhanced protective capacity of updated code provisions for steel moment-resisting frames in high-risk seismic zones.

Keywords: Demand and Capacity Factored Design (DCFD); Incremental Dynamic Analysis (IDA); Intermediate Steel Moment Resisting Frame; Ductility.

Nomenclature

A	intercept of the median IDA curve are derived in logarithmic space
B	The slope of the median IDA curve, derived in logarithmic space
D	seismic demand factor
C	median structural capacity (drift)
C/D	Capacity-to-Demand ratio
K_0	intercept of the seismic hazard curve, linear regression in logarithmic space
K	slope of seismic hazard curve, linear regression in logarithmic space
APE	Annual Probability of Exceedance
ASD	Allowable Stress Design
CP	Collapse Prevention performance level
DCFD	Demand and Capacity Factored Design
DM	Damage Measure
IDA	Incremental Dynamic Analysis
IM	Intensity Measure
LS	Life Safety performance level
LRFD	Load and Resistance Factor Design

How to cite this article:
S. Motaghed and V. Barzian, "Integrating structural uncertainty into demand and capacity factored design: A case study of existing moment-resisting steel structures," *International Journal of Reliability, Risk and Safety: Theory and Application*, vol. 9, no. 1, pp. 42-55, 2026, 10.22034/IJRRS.2026.9.1.4.

1. Introduction

Seismic performance assessment is a fundamental aspect of performance-based design and the retrofit of both new and existing structures [1-2]. Quantitative safety evaluation is essential for ensuring that structures perform adequately during earthquakes [3-4]. Jalayer (2003) introduced the probabilistic demand and capacity format (DCFD) as a framework for incorporating uncertainties in seismic performance evaluation [5]. Utilizing mathematical relationships, he proposed a practical approach for assessing structural safety. The DCFD method, which considers the critical ratio of demand to capacity as a direct global damage metric, facilitates intuitive interpretation and helps pinpoint the onset of prescribed performance levels. Jalayer et al. (2007) further expanded this approach by integrating it with Incremental Dynamic Analysis (IDA) and fragility curves to evaluate the seismic behavior of reinforced concrete structures [6].

The DCFD method has gained prominence due to its practicality and versatility across different structural systems and hazards. Vamvatsikos (2012) compared the power law approach and an innovative method for determining hazard curve coefficients to enhance the accuracy of results within the DCFD framework [7]. Jalayer et al. (2016) evaluated the effects of flooding on masonry structures using DCFD [8], while Miano et al. (2017) applied the method to assess rehabilitation strategies for earthquake-damaged concrete structures [9]. WeisMoradi and Darvishan utilized a probabilistic DCFD framework through OpenSEES to analyze the seismic performance of mega-braced BRB frames under near-fault earthquakes, demonstrating the method's effectiveness in ensuring high structural reliability [10]. Jalayer et al. (2020, 2021), DCFD utilizes intensity-based analysis to directly relate structural demand and capacity, allowing intuitive safety checks even with unscaled ground motion records [11-12]. Recent applications, such as those by Motaghed and Moghaddam (2024), have leveraged DCFD to evaluate confidence levels in existing Iranian RC moment-resisting frames, highlighting its efficacy in practical safety verification [13]. Other studies, including Mehrabi-Moghaddam et al. (2019) and Flores & Tolentino (2024), demonstrate DCFD's ability to estimate reliability and assess collapse prevention limits efficiently, often employing simplified or numerical integration approaches [14-15]. Ahmed & Tanoli (2025) further reinforce DCFD's value in risk-resilient retrofitting under performance-based frameworks [16]. Mehrabi Moghadam et al. (2022) and Motaghed et al. (2023 & 2024) evaluate the confidence level of existing moment-resisting reinforced concrete frames in Iran, showing that the structural performance confidence level decreases with increasing height, meaning taller frames have lower reliability [17-18,13]. Barzian et al. investigated how uncertainties in structural parameters affect the IDA response of intermediate steel moment-resisting frame structures [19].

Collectively, these works substantiate DCFD as a flexible and transparent tool for seismic performance evaluation and reliability assessment in structural engineering.

In this paper, we focus on the probabilistic seismic safety assessment of 12 medium-ductility steel moment-resisting frames, modeled in OpenSEES. These existing residential structures, varying in height (3, 5, and 8 stories) and span (3 and 5 bays), were designed according to different editions of the Iranian seismic code (Standard No.2800, third and fourth editions) and the National Building Code. By subjecting the frames to IDA using 20 suitable ground motion records, this study provides comprehensive and comparative safety boundaries based on the DCFD approach, contributing valuable data for the performance-based evaluation and design of steel structures.

2. Methodology: Probabilistic Demand Capacity Factored Design (DCFD) Framework

The Probability-Based Demand and Capacity Factor Design (DCFD) seismic framework, by incorporating uncertainties associated with various components involved in structural performance assessment and evaluation, provides corresponding relationships and coefficients. This format shares substantial similarity with the Load and Resistance Factor Design (LRFD) method, with the principal distinction being that the demand and capacity factors—derived from displacement parameters—replace load and resistance factors, which are force-based quantities. Moreover, uncertainties are extensively represented throughout the related expressions. The DCFD format is derived through a reformulation of the annual exceedance probability, supplemented with several methodological innovations.

The purpose of determining the third and fourth editions of this code is to obtain criteria and clauses for the design and implementation of buildings so that buildings do not suffer significant damage to their structure from the effects of earthquakes, while minimizing losses. However, these two editions differ in design concepts and some control criteria. Both editions use linear static analysis and have a similar risk level. However, in the third edition, the allowable stress method is used to design structures, while in the fourth edition, we see limit states in the design process. Now the question that is being considered is which edition has a higher seismic probability capability. To find out the answer to this question, we intend to design structures based on the criteria of these two codes and then examine the reliability of the two in a functional format. It should also be noted that this innovative format (DCFD) examines the performance of structures by considering the uncertainties resulting from the demand and capacity, which are broadly based on displacement relationships.

2.1 Definition of Performance Levels

In this study, two performance levels are considered: LS corresponding to an APE of 10% in 50 years and CP corresponding to an APE of 2% in 50 years.

The establishment or extension of any design format primarily requires the determination of an appropriate design criterion. A plausible design criterion for a structural system is that the APE of a specified limit state should be less than or equal to its allowable exceedance probability:

$$H_{LS} \leq P_0 \tag{1}$$

where

H_{LS}: the APE of the limit state, and

P_0: The allowable APE.

By substituting these terms and rearranging equation 1, along with applying appropriate mathematical simplifications and analytical innovations, the following expression for the DCFD format is derived:

$$\eta_{D|^{P_0}S_a} . e^{\frac{1k}{2b}\beta^2_{D|Sa}} \leq \eta_C . e^{-\frac{1k}{2b}\beta^2_C} \tag{2}$$

where

$\eta_{D|^{P_0}S_a}$: median demand

η_C : median capacity

$\beta^2_{D|S_a}$: standard deviation of demand due to uncertainties

β^2_C : standard deviation of capacity due to uncertainties

K: slope of the seismic hazard curve in logarithmic space

b: slope of the IDA curve in logarithmic space

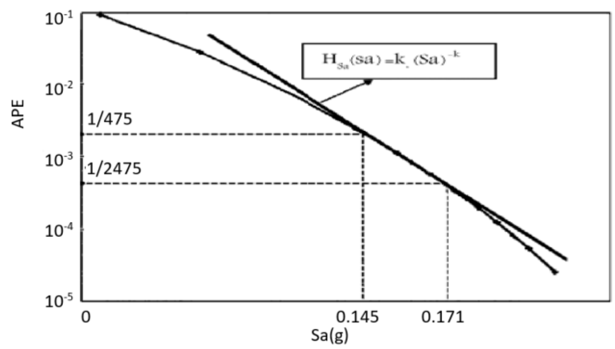

Figure 1. Linear estimation of seismic hazard curve, for a 3-story, 3-span structure, 4th edition

Figure 1 illustrates the linear fit of the seismic hazard curve for a 3-story, 3-span steel structure designed per the fourth edition. The seismic hazard data for Behbahan city, a high seismic hazard region, are utilized in this research [20-21]. The method for deriving coefficients k and k_0 in logarithmic coordinates is detailed in Figure 2. Consequently, given the target APE and the slope and intercept coefficients, the corresponding Sa value is obtained.

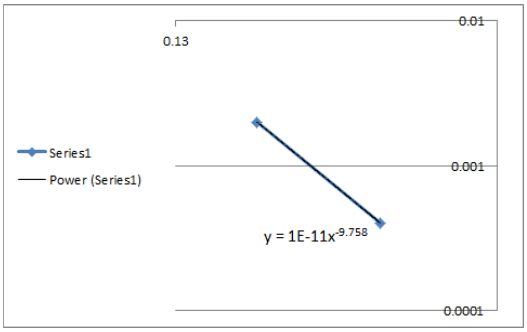

Figure 2. Linear estimation of the seismic hazard curve and obtaining the coefficients k and k_0, 3-story, 3-span structure, fourth edition, in logarithmic space based on the power law

Furthermore, by separating the uncertainties, the above relation can be expressed in the following form.

$$\eta_{D|^{P_0}S_a} . e^{\frac{1k}{2b}(\beta^2_{RD|Sa}+\beta^2_{UD|Sa})} \leq \eta_C . e^{-\frac{1k}{2b}(\beta^2_{RC}+\beta^2_{UC})} \tag{3}$$

where

$e^{\frac{1k}{2b}(\beta^2_{RD|Sa}+\beta^2_{UD|Sa})}$: the capacity factor resulting from epistemic and aleatory uncertainties and

$e^{-\frac{1k}{2b}(\beta^2_{RC}+\beta^2_{UC})}$: the demand factor resulting from epistemic and aleatory uncertainties is defined as follows:

The right-hand side of the equality is called the capacity factor, analogous to the resistance factor in the LRFD method. Similarly, the left-hand side of the equality is referred to as the demand factor for the allowable probability P_0, which corresponds to the load factor in LRFD. It is important to note that the demand factor depends on the acceptable probability level P_0, whereas the capacity factor does not. In contrast, neither factor in the LRFD method depends on the probability level P_0.

2.2 Demand factor based on displacement ($\eta_{D|^{P_0}S_a}$)

The expression $\eta_{D|^{P_0}S_a}$ represents the median demand based on displacement derived from the spectral acceleration corresponding to the spectral acceleration at the allowable annual exceedance probability. Figure 3 graphically illustrates the procedure for obtaining $\eta_{D|^{P_0}S_a}$. Moreover, the demand relation can be expressed as follows.

$$\eta_{D|^{P_0}S_a} = a(P_{0_{S_a}})^b = a\left(\frac{P_0}{K_0}\right)^{-\frac{b}{k}} \tag{4}$$

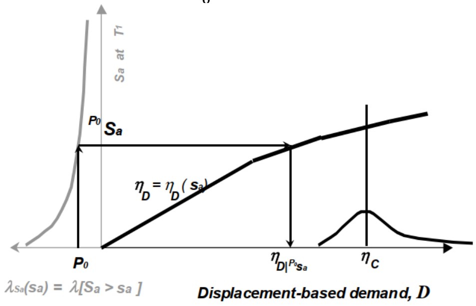

Figure 3. Schematic for determining the median demand and displacement-based capacity

where a is the intercept of the IDA curve in logarithmic space. As an example for parameter calculation, Figure 4 shows the parameters a and b estimation for the 3-story, 3-bay structure designed per the 4th edition.

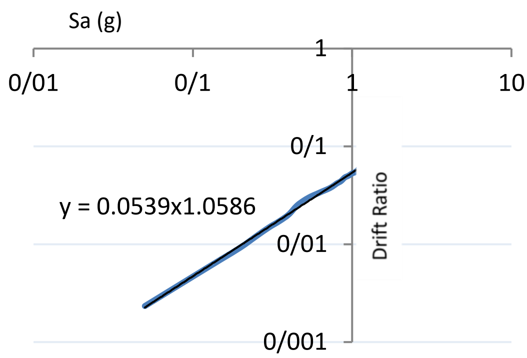

Figure 4. Parameters a and b for the 3-story, 3-bay steel structure designed per the 4th edition

2.3 Capacity based on displacement (η_C)

The median capacity is a displacement-based limit state that characterizes structural conditions, with various codes prescribing specific values for different performance level states. In this study, the values prescribed by the Iranian code 2800 are adopted for the life safety performance level. Moreover, since the collapse threshold performance criterion is not addressed in code 2800, this research employs the collapse prevention performance level as defined in FEMA 350 guidelines.

According to the Iranian seismic code (standard No. 2800), the median capacity at the LS performance level in the third edition is computed. For structures with periods less than 0.7 seconds, C=0.025, and for periods exceeding 0.7 seconds, C=0.02 is recommended [23]. Given that all structures analyzed under the third edition exceed 0.7 seconds, a median capacity of 0.02 is adopted.

In the fourth edition for the LS performance level, median capacities are calculated as 0.025 for 3- and 5-story buildings and 0.02 for structures taller than 5 stories (including the 8-story structures in this study). Since the CP performance level is not explicitly covered in code 2800, its median capacity is derived based on FEMA 350 guidelines [24].

2.4 Demand factor ($e^{\frac{1k}{2b}\beta^2{}_{D|S_a}}$)

The demand factor accounts for the uncertainties in the structural demand during calculations. The dispersion of the demand factor is denoted by $\beta_{D|S_a}$, which equals the standard deviation of the analyzed data on a logarithmic scale. The ratio $\frac{k}{b}$ represents the sensitivity of the probability of demand exceedance, where k is obtained from regression of the seismic hazard curve, and b is derived from Incremental Dynamic Analysis (IDA) in logarithmic space. Similar to the LRFD design approach, the demand factor is expressed exponentially as γ. Due to the exponential nature and the positive exponent of this expression, the demand factor is always greater than one.

In the DCFD framework, three uncertainties, including demand random uncertainty, demand model uncertainty, capacity random uncertainty, and capacity model uncertainty, are considered in the calculation process [25]. The demand random uncertainty (**β_{RD}**) is the standard deviation arising from seismic record variability [26]. The demand random uncertainty is estimated by fitting lognormal distributions to drifts analogous to spectral acceleration from Step 2. It is noted that other minor random uncertainties (e.g., damping variation, live load mass, material properties) are neglected due to their marginal impact. The demand model uncertainty (**β_{UD}**) is evaluated using the tables provided in FEMA 350, for example, Table 1 [27-30].

Table 1. lists parameters for demand model uncertainty (βUD) derivation [24]

	Analysis Procedure							
	Linear Static		Linear Dynamic		Nonlinear Static		Nonlinear Dynamic	
Performance Level	IO	CP	IO	CP	IO	CP	IO	CP
Type 1 Connections								
Low Rise (<4 stories)	0.17	0.22	0.15	0.16	0.14	0.17	0.10	0.15
Mid Rise (4 – 12 stories)	0.18	0.29	0.15	0.23	0.15	0.23	0.13	0.20
High Rise (> 12 stories)	0.31	0.25	0.19	0.29	0.17	0.27	0.17	0.25
Type 2 Connections								
Low Rise (<4 stories)	0.19	0.23	0.16	0.25	0.18	0.18	0.10	0.15
Mid Rise (4 – 12 stories)	0.20	0.30	0.17	0.33	0.14	0.21	0.13	0.20
High Rise (> 12 stories)	0.21	0.36	0.21	0.31	0.18	0.33	0.17	0.25

2.5 Capacity factor ($e^{-\frac{1k}{2b}\beta^{2}c}$)

The capacity factor, due to the negative exponent in its defining function, is a decreasing coefficient and is always less than or equal to one. Similar to the demand factor, it is used to account for uncertainties; however, it specifically considers the uncertainties associated with the structural capacity.

The capacity random uncertainty (**β_{RC}**) is taken as 0.3. The capacity model uncertainty β_{UC} is obtained by the approximate equation $\beta_{UC} = \sqrt{3} \times \beta_{UD}$ [32].

2.6 Determination of Confidence Level

Consequently, the capacity applied for design and control of the structure is always less than or equal to the median capacity that results from accounting for these uncertainties. Following the LRFD design approach, the capacity factor $\emptyset$ is expressed exponentially. Ultimately, the relation can be written as follows:

$$D.\ \gamma \leq C.\ \emptyset \tag{5}$$

where

D and C, respectively, represent the median displacement-based demand and capacity, while γ and $\emptyset$ denote their corresponding factors. It is evident that by satisfying the above relationship, the structure exhibits safe and acceptable performance. To determine the level of confidence, by substituting and simplifying the expressions derived from the exceedance of limit states, the following equations are ultimately obtained:

$$\frac{\eta_{D|S_a(P_{0S_a})} \cdot \gamma}{\eta_C \cdot \emptyset} \leq \lambda_x \tag{6}$$

$$\gamma = \gamma_R \cdot \gamma_U = e^{\frac{1k}{2b}\beta_{RD}^2} \cdot e^{\frac{1k}{2b}\beta_{UD}^2} \tag{7}$$

$$\emptyset = \emptyset_R \cdot \emptyset_U = e^{-\frac{1k}{2b}\beta_{RC}^2} \cdot e^{-\frac{1k}{2b}\beta_{UC}^2} \tag{8}$$

$$\lambda_x = e^{-\beta_{UT}(K_x - \frac{1k}{2b}\beta_{UT})} \tag{9}$$

λ_x: The confidence coefficient, based on a given confidence level x, and K_x is related to the Gaussian variance coefficient. By simplifying the relationship, the following equation can be ultimately derived:

$$\frac{\eta_{D|S_a(P_{0S_a})} \cdot \gamma_R}{\eta_C \cdot \emptyset_R} \leq e^{-K_x \beta_{UT}} \tag{10}$$

FEMA-350 recommends a confidence level exceeding 90% for the collapse prevention performance level. For the unrestricted serviceability level, 50% confidence is suggested, whereas no explicit recommendation is provided for Life Safety.

In this study, a conservative confidence level of 90% is adopted for both Life Safety (LS) and Collapse Prevention (CP) performance levels to ensure robustness.

Based on the above relationships, to achieve a desired confidence level for a structure at a given allowable exceedance probability, the following procedure can be followed:

1. Determine the demand factor corresponding to the allowable exceedance probability, as well as the capacity factor.
2. Calculate the ratio of the demand factor to the capacity factor.
3. Compute the standard deviation considering the total uncertainty ($\beta_{UT} = \sqrt{\beta_{UD}^2 + \beta_{UC}^2}$)
4. Calculate K_x
5. Finally, compute the confidence level corresponding to x. [33]

3. Modeling and Analysis

3.1 Structures

In this research, twelve structures of medium-ductility moment-resisting frames were modeled and analyzed using the ETABS software. Due to the absence of diagonal members, moment-resisting frames offer architectural freedom. Additionally, since all columns participate in resisting lateral loads, the load is transferred uniformly to the foundation. Moreover, given its high deformation capacity and ductility, the system absorbs energy within the frame, thereby increasing resistance against shear forces. Based on the plan illustrated in Figure 5, a three-dimensional model was first developed, from which a two-dimensional frame was extracted. Consequently, the analyzed frame represents a peripheral (environmental) frame. In this configuration, all peripheral frames—except for the first and last columns—and the beams connected to the internal columns, which are assumed pinned, are modeled as rigid members [34]. The 12 designed structures are as follows:

1. 3-story buildings with 3 and 5 spans, designed according to the third and fourth editions of Standard 2800 (a total of 4 models).
2. 5-story buildings with 3 and 5 spans, designed according to the third and fourth editions of Standard 2800 (a total of 4 models)
3. 8-story buildings with 3 and 5 spans, designed according to the third and fourth editions of Standard 2800 (a total of 4 models)

The modeling assumptions are shown in Figures 5-9, and the geometry of the structures is shown in Figures 10 - 16. The steel moment-resisting frames with moderate ductility are designed for residential use. Each story height is 3 m, and the tributary width of each frame is 4 m. The gravity load system consists of joist-slab floors. The middle bay of each frame spans 5 m, while the side bays span 4 m each. The structures are located in Behbahan city, which is characterized by high seismic hazard, and the soil profile is assumed to be of type II. The beams are composed of IPE sections, while the columns are fabricated from BOX sections. The steel grade used is ST37. Table 2 shows beams and column section properties.

Table 2. Sections of beams and columns

section								
column						beam		
NO	section	name	NO	section	name	NO	section	name
1	BOX300*25	C1	9	BOX240*15	C9	1	IPE450	B1
2	BOX300*20	C2	10	BOX200*15	C10	2	IPE400	B2
3	BOX350*25	C3	11	BOX200*12	C11	3	IPE360	B3
4	BOX270*25	C4	12	BOX180*15	C12	4	IPE330	B4
5	BOX270*20	C5	13	BOX180*12	C13	5	IPE300	B5
6	BOX250*25	C6	14	BOX150*12	C14	6	IPE270	B6
7	BOX250*20	C7	15	BOX150*10	C15			
8	BOX240*20	C8	16	BOX150*8	C16			

with the following material properties:
Unit weight: $\gamma_S = 7850\ kgf/m^3$
Modulus of elasticity: $E_S = 2 \times 10^6\ kgf/cm^2$
Minimum yield strength: $F_y = 2400\ kgf/cm^2$
Minimum ultimate tensile strength: $F_y = 3700\ kgf/cm^2$
And the Loading Assumptions are:
Dead load of floors: 570 kg/m²
Live load of floors: 200 kg/m²
Line dead load from exterior walls with cladding: 235 kg/m
Dead load of roof: 640 kg/m²
Live load of roof: 150 kg/m²
Line dead load from peripheral walls with cladding: 1200 kg/m
Response modification factors (R): 7 for the third edition, 5 for the fourth edition.

3.2 Modeling and Analysis Procedure

To model and analyze the structure, OpenSees software is employed due to its capability to perform linear and nonlinear analyses while accounting for hysteretic behavior. For this purpose, the selected hysteresis model must be capable of simulating the factors influencing structural behavior, including elastic and inelastic responses, plastic hinge formation, and collapse [35].

In this study, to account for stiffness degradation, strength deterioration, and local buckling effects, the concentrated plasticity model (plastic hinge) is utilized. In this approach, each beam or column member consists of one elastic beam or column element along with two plastic rotational springs with degrading behavior at the initial and terminal ends of the member, each having zero length. The structural analysis for solving the equations employs the slope-deflection method, equivalent stiffness, and deformations. In this method, the elastic beam is assigned a stiffness greater than its elastic stiffness, while the springs are assigned a stiffness less than rigid stiffness, which equivalently represents the behavior of the elastic member and the total initial state of the springs. In the nonlinear behavioral regime, the springs with degrading behavior provide highly accurate deformation due to degradation.

The characteristics of the rotational springs are determined based on the trilinear curves of the members and experimental studies [36]. The modified Ibarra-Krawinkler deterioration model is adopted in this research (Figure 5). As observed in Figure 1, these curves include a new branch that can also predict the strength loss after the residual strength. Additionally, to model the shear deformations of the connection panel zone—which has a significant impact on the linear and nonlinear inter-story drift of steel frames—the joint2D element is employed (Figure 6). In Figure 6, the central spring corresponds to the connection panel zone stiffness, which exhibits very high stiffness due to the use of box sections for the columns.

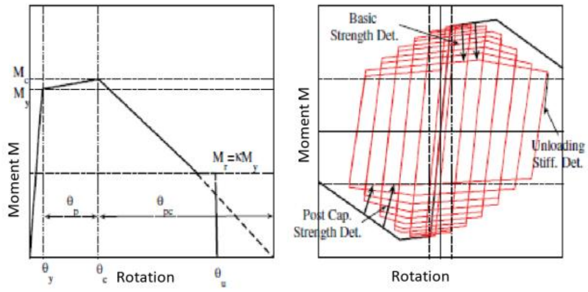

Figure 5. Modified Ibarra-Krawinkler deterioration model [35]

In Figure 5, Mye denotes the effective yield moment, Mp=E·Fy the product of the elastic modulus and yield strength (plastic moment), Mr the residual moment, θe the elastic deformation capacity, θp the plastic deformation, θcap the cap point deformation capacity, θrp the deformation at the onset of residual strength, and θpc the deformation capacity after the cap point.

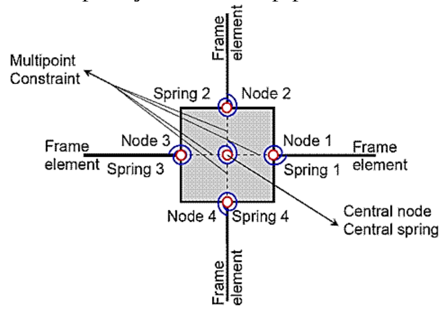

Figure 6. joint2D element for modeling connections in OpenSees software [37]

Considering P-delta effects is crucial in structural design and behavior assessment, as it is activated by applying lateral loads to the structure. In this study, the examined perimeter frames, depending on their tributary area, are subjected to P-delta effects. Since the internal columns of the three-dimensional structure are modeled as pinned, they do not resist specific shear forces under lateral loading and would collapse without connection to the moment frame. Therefore, the P-delta effect of these members is transferred to the moment frame. To incorporate these effects, a column with a pinned base connected to the target frame via pinned beams is added, where the tributary area of this column is half of the tributary area of the internal column beams (the other half is applied to the opposite perimeter frame). This column is referred to as a leaning column or lean column.

To validate the results obtained from nonlinear analyses, the modeling accuracy in the OpenSees software is verified. For this purpose, an 8-story steel frame with a special moment-resisting system, which was investigated in the studies by Elkady and Lignos [38], is modeled in OpenSees and subjected to nonlinear static pushover analysis using the first-mode lateral load pattern. As shown in Figure 3, the results from the modeling conducted in this research match those from the Elkady and Lignos studies.

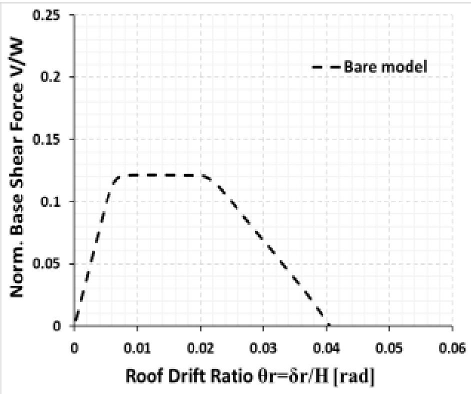

a. Elkady and Lignos[38]

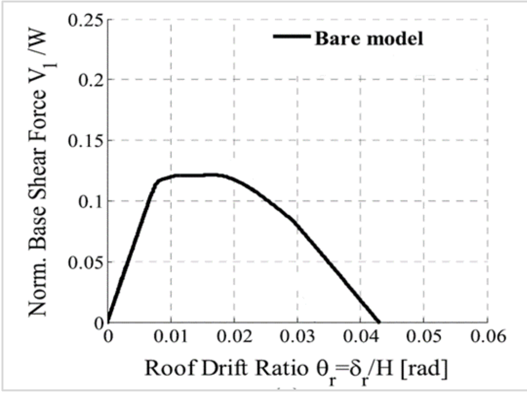

b. Modeling in this study

Figure 7. Comparison of modeling results in OpenSees software with the results from Elkady and Lignos studies for verification purposes

After structural modeling, the IDA was conducted using a suite of 20 recorded ground motions selected via the CMS method [11]. Selected earthquake ground motion records are shown in Table 3.

Table 3. Selected Earthquake Ground Motion Records

No.	Earthquake Event	Station	Distance (km)	Shear Wave Velocity (m/s)	PGA (g)	Magnitude (Mw)
1	Tabas longitudinal	Dayhook	13.94	659.6	0.3279	7.35
2	Manjil longitudinal	Abbar	12.56	742.0	0.5146	7.34
3	San Fernando-000	Pearblossom pump	39.98	529.1	0.1018	6.61
4	San Fernando-270	Pearblossom pump	38.97	529.1	0.1358	6.61
5	San Fernando-291	Lake hughes	22.57	670.8	0.1339	6.61
6	Kern county-111	Taft Lincoln School	38.89	385.4	0.1778	7.36
7	Morgan hill-067	Gilroy Gavilan Coll	14.84	729.7	0.1144	6.19
8	Coyote Lake -303	San Juan Bautista	19.70	370.8	0.1074	5.47
9	Friuli, Italy-000	Tolmezzo	15.82	424.8	0.3513	6.50
10	Oroville-132	Santa Barbara Court	24.60	482.5	0.1628	6.43
11	N. Palm Springs-090	Joshua Tree fire st	26.88	379.3	0.0651	6.06
12	Landers-000	Twentynine palms	41.43	684.9	0.0802	7.28
13	Landers-090	Twentynine palms	41.43	684.9	0.0603	7.28
14	Loma prieta-250	Anderson Dam downstream	20.26	488.8	0.2439	6.93
15	Loma prieta-000	Fremont Mission SJ	39.51	367.7	0.1244	6.93
16	Loma prieta-090	Fremont Mission SJ	39.51	367.6	0.1057	6.93
17	Loma prieta-225	San jose-santa	33.62	488.8	0.1164	6.93
18	Northridge 360	Alhambra – Fremont School	36.77	550.0	0.0798	6.69
19	Northridge 180	La crescenta – new york	18.50	446.0	0.1591	6.69
20	Northridge 070	La- chalon rd	20.45	740.1	0.2255	6.69

Spectral acceleration at the fundamental period of the structure was adopted as the Intensity Measure (IM), and the maximum inter-story drift ratio was chosen as the Damage Measure (DM).

To quantitatively express the vulnerability of various structural and non-structural components, the probability of occurrence or exceedance of a specific damage level can be expressed in terms of an intensity measure. Repeating this process for various values of the intensity measure results in generating normalized curves known as fragility curves.

After developing the structural models and performing incremental dynamic analysis (IDA), the engineering demand and capacity parameters can be obtained at different levels. Considering the structural uncertainties, different demand and capacity measures are derived under IDA, which can be evaluated and presented using fragility curves—probabilistic curves for a limit state. Fragility curves can be plotted for all limit states (immediate occupancy, life safety, near collapse, etc.). For instance, in the near-collapse limit state, the intensity measure at which the structure collapses (SCT) is used. This is the maximum intensity for which the dynamic analysis yields a convergent response, after which the IDA curve flattens. Thus, the number of IDA curves yields the corresponding number of structural collapse points. According to the conducted research, the lognormal distribution is the optimal and most suitable function for expressing the collapse fragility curve. Accordingly, the fragility curve is expressed by Equation (11).

$$P(Collapse \mid IM = im_i) = \Phi\left(\frac{LN(im_i) - LN(\eta_c)}{\beta_C}\right) \qquad (11)$$

In this equation, IM denotes the intensity measure (IMi represents the near-collapse intensity measure), μ the mean, β the standard deviation, and Φ the standard normal cumulative distribution function [39].

The location's distance from active fault rupture zones (more than 10 km). The moment magnitude of the selected seismic events ranged from 4.5 to 7.5, with peak ground acceleration (PGA) values between 0.05 g and 1 g. Considering the site soil type classified as II and based on provisions in Standard No. 2800, the shear wave velocity was assumed to be between 375 and 750 m/s.

4. Results and Discussion

To perform IDA, the structures designed in the previous section are modeled in OpenSees software and analyzed using the records introduced in Chapter 3. The results from the IDA of each structure are presented graphically. The 16th, 50th, and 84th percentiles are also obtained using the conditional relationship provided in Chapter 3, accounting for collapse effects, and are displayed as dashed lines.

In this research, the structural performance is evaluated at the life safety (LS) limit state and the near-collapse (CP) limit state. For this purpose, fragility curves are utilized, derived by fitting a normal distribution to the data obtained from IDA. The developed fragility curves have the maximum inter-story drift or spectral acceleration on the horizontal axis and the probability of exceeding the target limit states on the vertical axis, calculated as the cumulative area under the normal curve. The IDA results for the designed structures under the 20 considered ground motions, along with the 16th, 50th, and 84th percentiles, as well as the fragility curves for the collapse and life safety limit states, are illustrate.

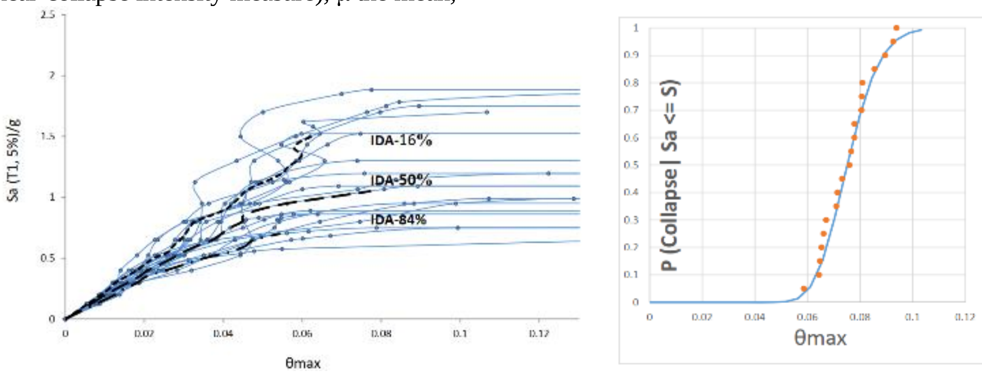

Figure 8. IDA curves and corresponding drift fragility curves for the collapse of the 3-story, 3-bay structure (4th edition)

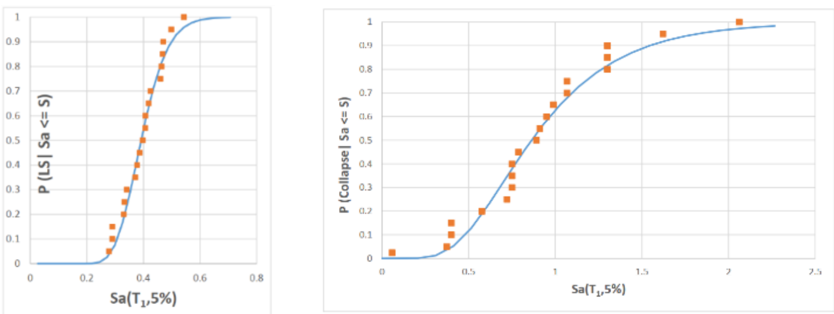

Figure 9. Spectral acceleration fragility curves for CP and LS levels of the 3-story, 3-bay structure (4th edition)

βRTRM: Standard deviation of demand (record-to-record variability), derived from the logarithmic distribution fitted to the drifts corresponding to spectral accelerations from the second part, followed by calculation of the standard deviation. Note that other random demand uncertainties, such as damping, live load mass, material properties, etc., are neglected due to their minor influence on the standard deviation [40].

Tables 4 and 5 summarize the seismic performance evaluation outcomes and reliability indices for the designed structures at LS and CP performance levels, respectively.

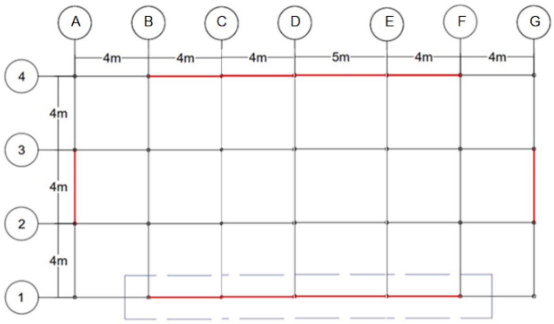

Figure 10. Plan of studied structures

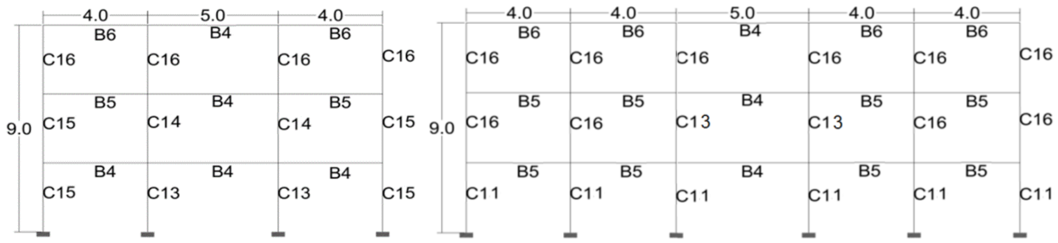

Figure 11. 3-Story Structures with 3 and 5 Spans, Third Edition of Standard 2800

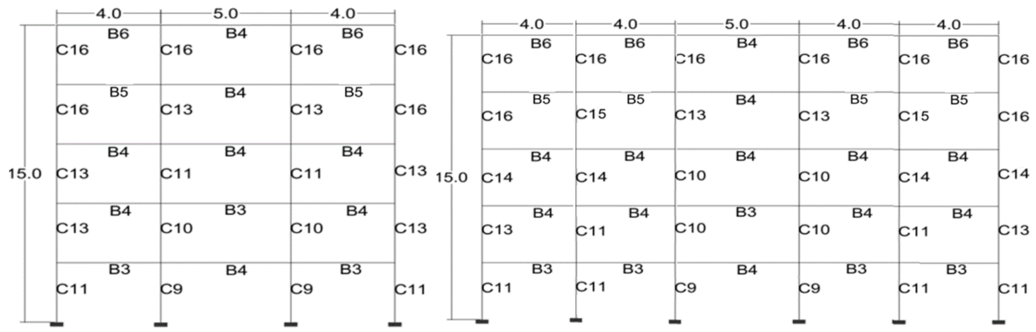

Figure 12. 5-Story Structures with 3 and 5 Spans, Third Edition of Standard 2800

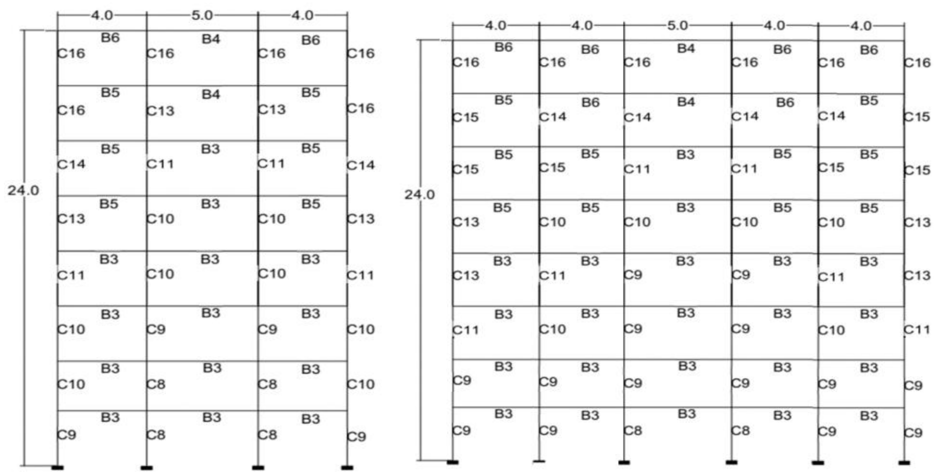

Figure 13. 8-Story Structures with 3 and 5 Spans, Third Edition of Standard 2800

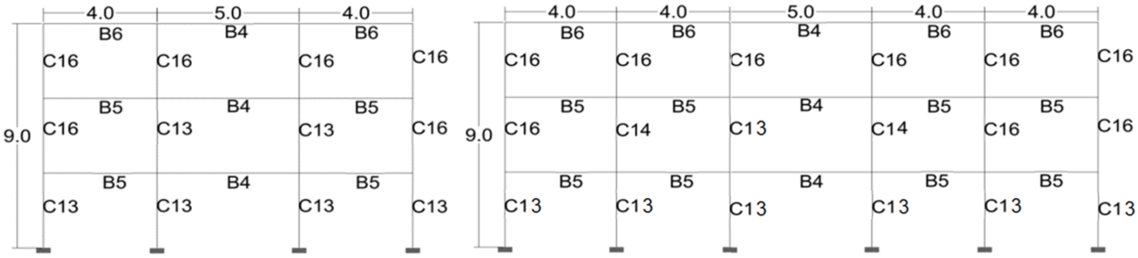

Figure 14. 3-Story Structures with 3 and 5 Spans, Fourth Edition of Standard 2800

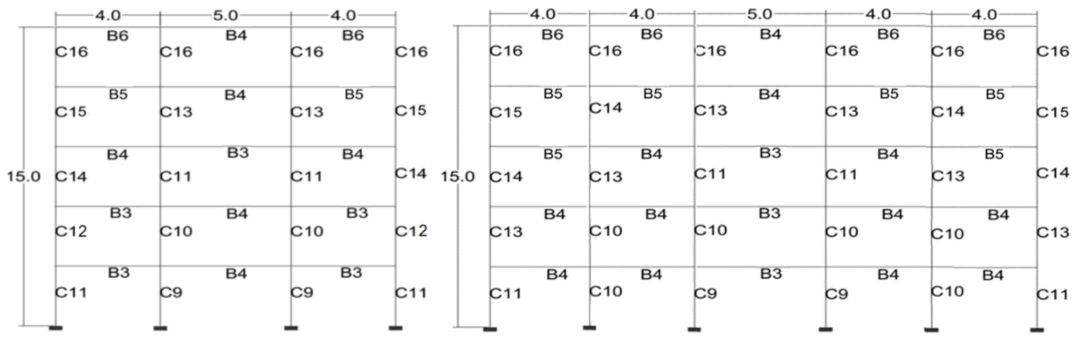

Figure 15. 5-Story Structures with 3 and 5 Spans, Fourth Edition of Standard 2800

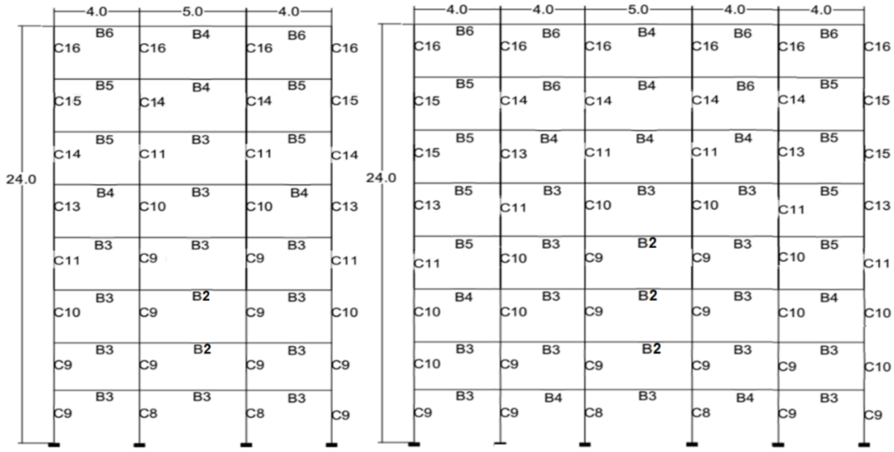

Figure 16. 8-Story Structures with 3 and 5 Spans, Fourth Edition of Standard 2800

Table 4. Seismic Performance Evaluation Results and Reliability Indices for Designed Structures at Life Safety (LS) Level

Code Edition	Structure Type	b	D	C	$\beta_{RD\|S_a}$	$C.\emptyset$	$D.\gamma$	$\frac{C.\emptyset}{D.\gamma} \geq 1$	λ_{con}	β_{UT}	X	X≥ 0.9
Third Edition 2800	3-story, 3-bay	1.103	0.00769	0.020	0.116	0.0110	0.0087	Pass	1.265	0.139	0.988	Safe
	3-story, 5-bay	1.070	0.00730	0.020	0.137	0.0108	0.00856	Pass	1.266	0.141	0.989	Safe
	5-story, 3-bay	1.115	0.00765	0.020	0.189	0.01000	0.00987	Pass	1.012	0.184	0.789	Not Safe
	5-story, 5-bay	1.073	0.00790	0.020	0.185	0.00973	0.01023	Not Pass	0.951	0.184	0.6890	Not Safe
	8-story, 3-bay	1.311	0.00764	0.020	0.323	0.01262	0.0108	Pass	1.16	0.218	0.898	Not Safe
	8-story, 5-bay	1.237	0.00800	0.020	0.312	0.01220	0.0114	Pass	1.06	0.214	0.819	Not Safe
Fourth Edition 2800	3-story, 3-bay	1.058	0.00840	0.025	0.161	0.01340	0.01020	Pass	1.320	0.167	0.999	Safe
	3-story, 5-bay	1.046	0.00720	0.025	0.125	0.01330	0.00830	Pass	1.594	0.14	0.995	Safe
	5-story, 3-bay	1.053	0.00800	0.025	0.136	0.01200	0.00970	Pass	1.230	0.179	0.972	Safe
	5-story, 5-bay	1.182	0.00730	0.025	0.207	0.01300	0.00965	Pass	1.346	0.187	0.989	Safe
	8-story, 3-bay	1.141	0.00790	0.020	0.278	0.01170	0.01096	Pass	1.075	0.203	0.935	Safe
	8-story, 5-bay	1.237	0.00796	0.020	0.301	0.01200	0.01120	Pass	1.075	0.210	0.830	Not Safe

Table 5. Seismic Performance Evaluation Results and Reliability Indices for Designed Structures at Collapse Prevention (CP) Level

Code Edition	Structure Type	b	D	C	$\beta_{RD \mid S_a}$	$C.\emptyset$	$D.\gamma$	$\frac{C.\emptyset}{D.\gamma} \geq 1$	λ_{con}	β_{UT}	X	X≥ 0.9
Third Edition 2800	3-story, 3-bay	1.10	0.0093	0.070	0.108	0.04768	0.0108	Pass	4.38	0.097	1	Safe
	3-story, 5-bay	1.07	0.0089	0.0677	0.130	0.0392	0.01065	Pass	3.686	0.128	1	Safe
	5-story, 3-bay	1.11	0.0094	0.073	0.199	0.0417	0.0129	Pass	3.22	0.161	1	Safe
	5-story, 5-bay	1.03	0.0101	0.074	0.209	0.0338	0.01396	Pass	2.42	0.204	0.999	Safe
	8-story, 3-bay	1.31	0.0104	0.0668	0.321	0.03695	0.0152	Pass	2.42	0.265	0.999	Safe
	8-story, 5-bay	1.23	0.0159	0.0657	0.312	0.0350	0.0234	Pass	1.49	0.263	0.998	Safe
Fourth Edition 2800	3-story, 3-bay	1.05	0.01016	0.070	0.159	0.0512	0.01261	Pass	4.066	0.096	1	Safe
	3-story, 5-bay	1.046	0.0087	0.080	0.126	0.0527	0.0103	Pass	5.07	0.099	1	Safe
	5-story, 3-bay	1.05	0.00976	0.083	0.149	0.0457	0.0127	Pass	3.6	0.154	1	Safe
	5-story, 5-bay	1.18	0.0092	0.074	0.218	0.0415	0.0128	Pass	3.24	0.176	1	Safe
	8-story, 3-bay	1.14	0.0104	0.0664	0.278	0.02688	0.0149	Pass	1.79	0.319	0.999	Safe
	8-story, 5-bay	1.23	0.01060	0.0662	0.301	0.0302	0.0155	Pass	1.90	0.300	0.999	Safe

Based on the results presented in Table 4, the seismic performance of structures designed according to the third and fourth editions of the Iranian Code 2800 at the Life Safety (LS) level indicates notable improvements in reliability under the updated standard. For the third edition, 3-story models generally satisfied performance criteria, achieving acceptable reliability indices ($\beta \approx 1.26$) and being classified as safe. However, higher-story structures, particularly the 5- and 8-story frames, showed reduced safety margins, with several models failing to meet the reliability threshold. In contrast, the fourth edition exhibits a consistent enhancement in seismic reliability across all configurations. All 3- and 5-story structures satisfied the LS performance criteria with improved reliability indices (β up to 1.59), reflecting the efficacy of the revised design provisions. Only the 8-story, 5-bay frame marginally failed to meet the safety requirement, suggesting that taller structures remain more vulnerable under seismic loading despite the code enhancements.

The results in Table 5 demonstrate that all structures designed according to both the third and fourth editions of Code 2800 successfully achieved the Collapse Prevention (CP) performance level. For every model analyzed, including those with increased story and bay counts, performance criteria were met, and reliability indices remained consistently high (β ranging from approximately 1.49 to 5.07), indicating substantial seismic safety margins compared to the Life Safety (LS) level evaluation. Notably, the fourth edition led to even higher reliability in several configurations, particularly for the 3- and 5-story buildings, reflecting improvements in the code provisions for collapse resistance. The seismic performance evaluation confirms that, at the CP level, both editions of the code provide sufficient safety across all assessed building configurations, with reliability indices approaching or reaching unity, highlighting the adequacy of contemporary design standards in preventing structural collapse during severe seismic events.

Based on Tables 4 and 5, structures with 3 stories and 3 or 5 bays, designed per either the third or fourth edition, generally demonstrate satisfactory performance and acceptable reliability indices. Structures designed according to the fourth edition (LRFD) consistently exhibit better performance and higher reliability than their third edition (ASD) counterparts. For the 5-story, 3-bay frame designed per the third edition, performance levels are acceptable; however, the reliability index is marginally insufficient, whereas the fourth edition design achieves satisfactory reliability. The 5-story, 5-bay frame does not meet target performance or reliability levels under the third edition but satisfies these criteria under the fourth edition.

According to the results obtained at the LS level, the 3-story, 3-span, and 5-span structures have acceptable performance and reliability levels. The fourth edition (LRFD) structures have better performance and higher reliability levels than the third edition (ASD) structures. In the 5-story, 3-span structure of the third edition, the acceptable performance is 1.012, but the inadequate reliability level is 0.789; for the fourth edition structure, the performance is 1.23, and the acceptable reliability level is 0.972, which is higher than that of the third edition. In the 5-story, 5-span structure, the functional safety status and reliability level are not met, which are recorded as 0.951 and 0.689, respectively. This is while in the fourth edition, the performance and reliability levels are high, which are recorded as 1.346 and 0.989, respectively.

Both the 8-story, 3-span structures of the third and fourth editions have performed safely, but the performance level of the third edition is lower than the target performance (0.898), while the fourth edition structure has a high performance level (0.935). In the 8-story, 5-span structure, both editions have performed safely, but their target performance level has not reached the target value, which is recorded as 0.819 in the third edition and 0.83 in the fourth edition. According to the results obtained, all structures are safe at the CP level and have a high level of reliability. In general, with the exception of one case, the reliability level of the fourth edition structures is higher than that of the third edition.

Notably, the mid-capacity drift values recommended by the code (0.02 in the third edition versus 0.025 in the fourth) significantly affect attained performance and reliability. For taller 8-story frames, both editions ensure structural safety, but the third edition yields lower reliability indices compared to the fourth. The 8-story, 5-bay frame performs safely under both editions but does not fully meet target reliability levels.

All evaluated structures demonstrate satisfactory safety and high reliability at the CP level. Apart from one exception, reliability indices are higher for structures designed according to the fourth edition compared to those of the third edition.

5. Conclusion

This study integrated structural uncertainty into the Demand Capacity Factored Design framework to assess the seismic safety of steel moment-resisting frames designed per both the third (ASD) and fourth (LRFD) editions of the seismic code 2800, considering the high seismic hazard context of Behbahan. Key findings include:

- The fourth edition designs exhibit improved seismic performance and reliability compared to the third edition, attributable in part to differences in prescribed capacity (drift limits) and response modification factors.
- Structures with fewer stories and bays consistently meet performance and reliability targets at the Life Safety level, while taller and more complex frames require the enhanced criteria of the fourth edition to reach acceptable safety margins.
- At the Collapse Prevention level, all structures satisfactorily achieve performance objectives, with the fourth edition designs generally offering higher assurance.
- The probabilistic framework utilizing IDA with a comprehensive suite of earthquake records effectively captures structural demand uncertainties and supports reliability-based decision-making.

These outcomes reinforce the suitability of the fourth edition seismic code provisions for ensuring robust seismic safety in steel frames within high-risk seismic zones and highlight the value of explicitly incorporating structural uncertainties into the design evaluation process.

Acknowledgments

We thank the Center of Monitoring Assessment and Prediction of natural disasters (MAP) of Behbahan Khatam Alanbia University of Technology.

Conflict of interest

No conflict of interest has been expressed by the authors.

6. References

[1] P. K. V. R. Padalu and M. Surana, "An overview of performance-based seismic design framework for reinforced concrete frame buildings," *Iranian Journal of Science and Technology, Transactions of Civil Engineering*, vol. 48, no. 2, pp. 635-667, 2024, https://doi.org/10.1007/s40996-023-01217-4.

[2] S. Motaghed and L. Emadali, "Performance-based methodology for seismic design and evaluation of bridges," *Advance Researches in Civil Engineering*, vol. 6, no. 1, pp. 1-13, 2025, https://doi.org/10.30469/arce.2025.511561.1084.

[3] A. Yazdani, S. Motaghed, and A. Mehrabi Moghadam, "Evaluation of seismic risk effect on total reliability index of structures, case study of concrete flexible frame frames," *Asas Journal*, vol. 18, no. 43, pp. 26-37, 2016, (in Persian).

[4] S. Motaghed and M. S. Shahidzade, "Seismic evaluation of steel I-girder bridges," *Journal of Applied Sciences*, vol. 11, no. 1, pp. 104-110, 2011, https://doi.org/10.3923/jas.2011.104.110.

[5] F. Jalayer and C. A. Cornell, "A technical framework for probability-based demand and capacity factor (DCFD) seismic formats," Pacific Earthquake Engineering Research Center, University of California, Berkeley, Rep. PEER Report 2003-08, 2003, https://peer.berkeley.edu/publications/2003-08.

[6] F. Jalayer, P. Franchin, and P. E. Pinto, "A scalar damage measure for seismic reliability analysis of RC frames," *Earthquake Engineering and Structural Dynamics*, vol. 36, pp. 2059–2079, 2007, https://doi.org/10.1002/eqe.704.

[7] D. Vamvatsikos and M. Fragiadakis, "Incremental dynamic analysis for estimating seismic performance sensitivity and uncertainty," *Earthquake Engineering and Structural Dynamics*, vol, 39, no. 2, 2010, pp. 141-163, https://doi.org/10.1002/eqe.935.

[8] F. Jalayer, S. Carozza, R. De Risi, G. Manfredi, and E. Mbuya, "Performance-based flood safety-checking for nonengineered masonry structures," *Engineering Structures*, vol. 106, pp. 109-123, 2016, https://doi.org/10.1016/j.engstruct.2015.10.007.

[9] F. Miano, F. Jalayer, H. Ebrahimian, A. Prota, and G. Manfredi, "Cloud analysis considering global dynamic instability," *16th World Conference on Earthquake Engineering*, Santiago Chile, 2017, Paper *N° 4789*.

[10] S. Veismoradi and E. Darvishan, "Probabilistic seismic assessment of mega buckling-restrained braced frames under near-fault ground motions," *Earthquakes and Structures*, vol. 15, no. 5, pp. 487-https://doi.org/10.12989/eas.2018.15.5.487.

[11] F. Jalayer, H. Ebrahimian, and A. Miano, "Intensity-based demand and capacity factor design: A visual format for safety checking," *Earthquake Spectra*, vol. 36, no. 4, pp. 1952-1975, 2020, https://doi.org/10.1177/8755293020919451.

[12] F. Jalayer, H. Ebrahimian, and A. Miano, "Record-to-record variability and code-compatible seismic safety-checking with limited number of records," *Bulletin of Earthquake Engineering*, vol. 19, no. 15, pp. 6361-6396, 2021, https://doi.org/10.1007/s10518-020-01024-6.

[13] S. Motaghed and A. M. Moghaddam, "Confidence level for Iranian existing moment resisting RC structures based on demand and capacity factored design method," *International Journal of Reliability, Risk and Safety: Theory and Application*, vol. 7, no. 1, pp. 93-102, 2024, https://doi.org/10.22034/IJRRS.2024.7.1.11.

[14] A. Mehrabi-Moghaddam, S. Motaghed, A. Yazdani, and A. Mehrabi-Moghaddam, "Seismic assessment of collapse prevention limit-state of RC structures using numerical integration method," in *Proceeding of 11th National Congress on Civil Engineering*, Shiraz, Iran, 2019.

[15] R. B. Flores and D. Tolentino, "Simplified estimation of reliability in structures subjected to seismic loads using the demand-capacity ratio format," *Bulletin of Earthquake Engineering*, vol. 22, no. 9, pp. 4635-4655, 2024, https://doi.org/10.1007/s10518-024-01923-y.

[16] H. A. Ahmed and W. A. Tanoli, "Seismic retrofitting of RC buildings using a performance-based approach for risk resilience and vulnerability assessment," *Buildings*, vol. 15, no. 8, p. 1333, 2025, Art. no. 1333, https://doi.org/10.3390/buildings15081333.

[17] A. Mehrabi Moghadam, A. Yazdani, and S. Motaghed, "Considering the yielding displacement uncertainty in reliability of mid-rise R.C. structures," *Journal of Rehabilitation in Civil Engineering*, vol. 10, no. 3, pp. 141-157, 2022, https://doi.org/10.22075/jrce.2021.19660.1376.

[18] S. Motaghed, A. Mehrabi Moghaddam, and N. Moayyeri, "Reliability of Iranian existing residential reinforced concrete structures in seismic events," *International Journal of Reliability, Risk and Safety: Theory and Application*, vol. 6, no. 2, 2023, pp. 55-64, https://doi.org/10.22034/ijrrs.2023.6.2.7.

[19] V. Barzian, S. Motaghed, A. Mehrabi Moghaddam, S. A. Asghari Pari, and L. Emadali, "Investigation the effect of structural parameters uncertainty on the response of incremental dynamic analysis of intermediate steel moment resisting frame structures," *Journal of Structural and Construction Engineering*, vol. 9, no. 10, pp. 175–195, 2022, (in Persian), https://doi.org/10.22065/jsce.2022.311616.2612.

[20] S. Motaghed, A. Nakhlian, L. Emadali, H. Mahmudian, and N. Eftekhari, "An overview of the seismic activity in Behbahan city, southwest Iran," *Advance Researches in Civil Engineering*, vol. 6, no. 2, pp. 50-64, 2024, https://doi.org/10.30469/arce.2025.519969.1086.

[21] S. Motaghed, A. Nakhlian, L. Emadali, N. Eftekhari, and H. Mahmoudian, "Seismic hazard assessment using arithmetic-weighted overlay method based on earthquake potential index (EPI), the southwestern Iran," *Iranian Journal of Remote Sensing & GIS*, vol. 17, no. 1, pp. 23-40, 2023, (in Persian), https://doi.org/10.48308/gisj.2023.229646.1133.

[22] S. Motaghed, N. Eftekhari, A. Nakhlian, L. Emadali, and H. Mahmoudian, "Seismic risk analysis in the Behbahan urban decay," *Safe City*, vol. 8, no. 3, pp. 1-15, 2024, (in Persian), https://doi.org/10.22034/ispdrc.2024.2036864.1122.

[23] "Iranian Code of Practice for Seismic Resistant Design of Building," Building and Housing Research Center, Tehran, Iran, Standard no. 2800, 2015, 4th Ed.

[24] "Recommended seismic evaluation and upgrade criteria for existing welded steel moment-frame buildings," SAC Joint Venture, Federal Emergency Management Agency, Washington, Rep. FEMA-351, 2000.

[25] S. Motaghed, A. Nakhlian, L. Emadali, N. Eftekhari, and H. Mahmudian, "Determining the natural frequency of Behbahan city soil using microtremor data analysis," *Journal of Geography and Environmental Hazards*, vol. 12, no. 4, pp. 233-251, 2024, (in Persian), https://doi.org/10.22067/geoeh.2023.80563.1326.

[26] S. Motaghed and A. Reza Fakhriyat, "Uncertainties in seismic hazard assessment of Metropolitan Tehran," *International Journal of Reliability, Risk and Safety: Theory and Application*, vol. 8, no. 1, pp. 1-11, 2025, https://doi.org/10.22034/IJRRS.2025.8.1.1.

[27] A. Miano, H. Sezen, F. Jalayer, and A. Prota, "Probability based comparison of retrofit methods for existing nonductile concrete frames," in *4th Conference on Smart Monitoring, Assessment and Rehabilitation of Civil Structures (SMAR)*, Zurich, Switzerland, 2017.

[28] A. B. Liel, C. B. Haselton, G. G. Deierlein, and J. W. Baker, "Incorporating modeling uncertainties in the assessment of seismic collapse risk of buildings," *Structural Safety*, vol. 31, no. 2, pp. 197–211, 2009, https://doi.org/10.1016/j.strusafe.2008.06.002.

[29] D. Vamvatsikos, "Accurate application and second-order improvement of SAC/FEMA probabilistic formats for seismic performance assessment," *Journal of Structural Engineering*, vol. 140, no. 2, 2012, https://doi.org/10.1061/(ASCE)ST.1943-541X.0000774.

[30] F. Jalayer, "Visualizing the demand and capacity factor design (DCFD) format for safety-checking," in *11th U.S. National Conference on Earthquake Engineering*, Los Angeles, USA, 2018.

[31] "Prestandard and Commentary for the Seismic Rehabilitation of Buildings: Rehabilitation Requirements," American Society of Civil Engineers, Washington, USA, Rep. FEMA 356, 2000.

[32] A. Yazdani, A. Mehrabi Moghaddam, and M.S. Shahidzadeh, "Parametric assessment of uncertainties in reliability index of reinforced concrete MRF structures using incremental dynamic analysis," *Amirkabir Journal of Civil Engineering*, vol. 49, no, 4, pp. 755-768, 2018, https://doi.org/10.22060/ceej.2016.707.

[33] S. Motaghed, A. R. Fakhriyat, M. S. Shahidzadeh, and N. Eftekhari, " Performance-based probabilistic seismic hazard analysis incorporating fault-specific minimum magnitude," *Earthquake Engineering and Resilience*, vol. 5, no. 2, pp. 148-168, 2026, https://doi.org/10.1002/eer2.70040.

[34] L. Emadali and S. Motaghed, "The use of differential interferometric synthetic aperture radar (DInSAR) technique for determining the displacement field caused by the March 28, 2025 Myanmar earthquake (Mw 7.7)," *Journal of Tectonics*, vol. 7, no. 28, pp. 67-78, 2025, (in Persian), https://doi.org/10.22077/jt.2025.9696.1207.

[35] D. Lignos, "Collapse of deteriorating structural systems under seismic excitations," Ph.D. dissertation, Deptartment of Civil and Environmental Engineering, Stanford University, Stanford, USA, 2008.

[36] A. Nicknam, M. Farhangdoust, A. Mazarei, and M. Ganjvar, "Seismic design parameters assessment of special steel moment resisting frames using the collapse margin ratio (CMR) method," *Amirkabir Journal of Civil Engineering*, vol. 50, no. 2, pp. 335–354, pp. 335-354, 2018, https://doi.org/10.22060/ceej.2017.11866.5091.

[37] A. Altoontash, "Simulation and damage models for performance assessment of reinforced concrete beam-column joints," Ph.D. dissertation, Deptment of Civil and Environmental Engineering, Stanford University, Stanford, USA, 2004.

[38] N. Shome and C. A. Cornell, "Probabilistic seismic demand analysis of nonlinear structures," Stanford University, Stanford, USA, Rep. RMS-35, 1999.

[39] A. Elkady and D. G. Lignos, "Modeling of the composite action in fully restrained beam to column connections: Implications in the seismic design and collapse capacity of steel special moment frames," *Earthquake Engineering and Structural Dynamics*, vol. 43, no. 13, pp. 1935–1954, 2014, https://doi.org/10.1002/eqe.2430.

[40] S.Y. Yun, R.O. Hamburger, C.A. Cornell, and D.A. Foutch, "Seismic performance evaluation for steel moment frames" *Journal of Structural Engineering*, vol. 128, no. 4, 2002, Art. no. 534, https://doi.org/10.1061/(ASCE)0733-9445(2002)128:4(534).